

Heavy-flavour production in ALICE at the LHC

S. Masciocchi for the ALICE Collaboration

EMMI and GSI Helmholtzzentrum fuer Schwerionenforschung GmbH, Darmstadt, Germany

Abstract

ALICE at the LHC is the experiment dedicated to study the physics of nucleus-nucleus collisions. The apparatus is well suited for the measurement of heavy-quark hadron production, making use of the high spatial resolution provided by the tracking detectors and the excellent particle identification, which are distinctive of the ALICE apparatus.

Results from proton-proton collisions at $\sqrt{s} = 2.76$ and 7 TeV, and from Pb–Pb collisions at $\sqrt{s_{NN}} = 2.76$ TeV are presented. The measurements in pp collisions provide an important test of perturbative QCD predictions. The precise vertex reconstruction together with the electron identification, allows the separation of the charm and the beauty components. Furthermore, the pp results are essential as a reference for the measurements in heavy-ion collisions. Nuclear modification factors were measured for D mesons, for electrons and for muons from heavy-flavour hadron decays. The elliptic flow of D mesons is also discussed. These measurements are important because they will provide information on the Quark-Gluon Plasma produced in heavy-ion collisions, via the energy loss of the heavy partons in the strongly interacting medium, and hints on the medium thermalization.

Keywords: Heavy-ion collisions, heavy-flavour production, energy loss, ALICE

1. Introduction

Heavy quarks, charm and beauty, are excellent probes to investigate quantum chromodynamics (QCD) processes in hadronic interactions, and to characterize the deconfined medium produced in high-energy heavy-ion collisions, the Quark-Gluon Plasma (QGP). Because of the large quark masses, heavy-flavour production proceeds mainly through initial hard parton-parton scattering. In proton-proton collisions, therefore, the production cross sections of charm and beauty quarks provide a test of perturbative QCD (pQCD). They also provide a crucial baseline for corresponding measurements in heavy-ion collisions. In such collisions a strongly interacting medium is formed, in which heavy quarks interact, after having been produced in the very initial stage of the collision. Consequently, heavy quarks experience the whole history of the medium evolution: they lose energy while propagating through the medium, and they might participate in the collective dynamics. A measurement of the azimuthal anisotropy of the charm hadron production and their elliptic flow (v_2) will give information on the charm thermalization in the medium.

A sensitive observable to characterize the effect of the dense medium on the heavy-quark production is the nuclear modification factor R_{AA} . This is defined as:

$$R_{AA}(p_t) = \frac{1}{\langle T_{AA} \rangle} \times \frac{dN_{AA}/dp_t}{d\sigma_{pp}/dp_t} \quad (1)$$

Email address: s.masciocchi@gsi.de (S. Masciocchi for the ALICE Collaboration)

where dN_{AA}/dp_t is the transverse momentum spectrum measured in heavy-ion (A–A) collisions, $d\sigma_{pp}/dp_t$ is the p_t -differential cross-section measured in pp collisions, and the ratio is scaled by the nuclear overlap function $\langle T_{AA} \rangle$ estimated through the Glauber model [1].

ALICE (A Large Ion Collider Experiment) at the LHC is the experiment dedicated to study the physics of nucleus-nucleus collisions. It is particularly well equipped to measure heavy-flavour hadrons in different decay channels. At mid-rapidity, detectors in the central barrel, in a uniform magnetic field of 0.5 T, provide high resolution track and vertex reconstruction, and precise particle identification for hadrons and for electrons. At forward-rapidity, a muon spectrometer offers triggering and precise tracking of muons. A complete description of the experiment can be found in [2]. The heavy-flavour physics program of ALICE includes the following channels:

- semi-electronic decays studied via inclusive electron spectra measured at mid-rapidity;
- semi-muonic decays at forward-rapidity;
- full reconstruction of hadronic decay channels of charm mesons and baryons at mid-rapidity.

These will be described in the Sections 2, 3, and 4, respectively. Results from both collision systems, proton-proton and Pb–Pb, at various center of mass energies will be presented and discussed.

2. Semi-leptonic decays of heavy-flavour hadrons at mid-rapidity

One method to measure the production of heavy-flavour hadrons consists in detecting the lepton produced in their semi-leptonic decays and analyzing the inclusive lepton transverse momentum spectrum. Semi-leptonic decays offer the advantage of a relatively large branching ratio, of the order of 10% for both charm and beauty hadrons.

At mid-rapidity (extending from ± 0.5 to ± 0.8 depending on the detector used in the measurement), electrons can be identified with high purity by a number of Particle IDentification (PID) detectors. The central PID device used in all approaches is the Time Projection Chamber (TPC), where the particle specific energy loss dE/dx is measured. The particle dE/dx as a function of the track momentum is shown in Fig. 1 (top). The ambiguities at low momentum, where the electron, kaon, proton and deuteron lines cross, are resolved using information from the Time-of-Flight (TOF) detector. At higher momenta, other detectors such as the Transition Radiation Detector (TRD) or the ElectroMagnetic Calorimeter (EMCal) help suppressing the hadron contamination.

The inclusive electron spectrum contains contributions from many sources other than the heavy-flavour hadron decays. The most important are: Dalitz decays of light neutral mesons (π^0 , η , ω , η' , ϕ), photon conversions in the beam pipe and detector material, di-electron decays of vector mesons (ρ , ω , ϕ), heavy quarkonia, and direct radiation.

In a first approach, the spectrum composed by these background electrons is described by the so-called electron cocktail (see [3] for an extensive description of this method), which is statistically subtracted from the inclusive spectrum. This approach was used to obtain the production cross section of electrons from charm and beauty hadron decays in pp collisions at $\sqrt{s} = 7$ TeV, shown in Fig. 2. Minimum bias events, for an integrated luminosity of 2.6 nb^{-1} , were used. The measurement is combined with a similar one by the ATLAS Collaboration [4], and compared to a pQCD calculation at fixed order with next-to-leading-log resummation (FONLL [5, 6, 7]). The theory prediction describes well the measurements over a very wide momentum range.

The combination with the ATLAS measurement helps to highlight one of the most important features of the ALICE apparatus, the capability to extend measurements to very low momenta, region in which a large part of the interesting physics resides, since the production cross section is largest. In fact, only by extending the measurement down to 0.5 GeV/c, can ALICE access $\approx 50\%$ of the total charm cross section, and $\approx 90\%$ of the beauty cross section, assuming FONLL transverse momentum shapes.

This measurement treats inclusively the contributions from both charm and beauty hadrons. The separation of the pure beauty component is achieved with two different analyses: one is based on the azimuthal angular correlations of the electron with hadrons produced in its vicinity, and the second one on the larger separation of the electron from the primary vertex for beauty hadron decays, because of their longer lifetime compared to charm and other sources.

The former analysis exploits the fact that the width of the near side correlation distribution is larger for beauty hadrons compared to charm hadrons, due to different decay kinematics of the hadrons themselves [8]. By fitting the angular correlations measured in pp collisions at $\sqrt{s} = 2.76$ TeV, the relative beauty contribution to the heavy-flavour

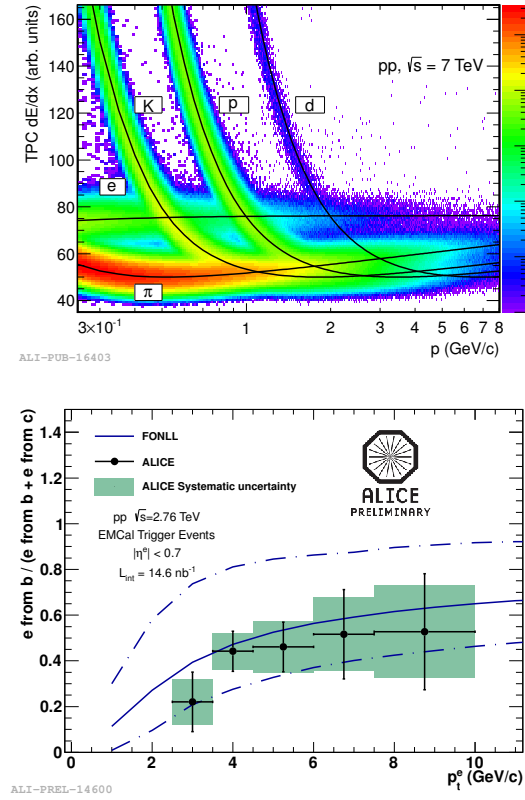


Figure 1: (Top) Specific energy loss dE/dx of charged tracks in the ALICE TPC (taken from [3]). Hadrons and electrons can be clearly identified. (Bottom) Relative beauty contribution to the heavy-flavour electron yield, in pp collisions at $\sqrt{s} = 2.76$ TeV, compared with FONLL pQCD calculations.

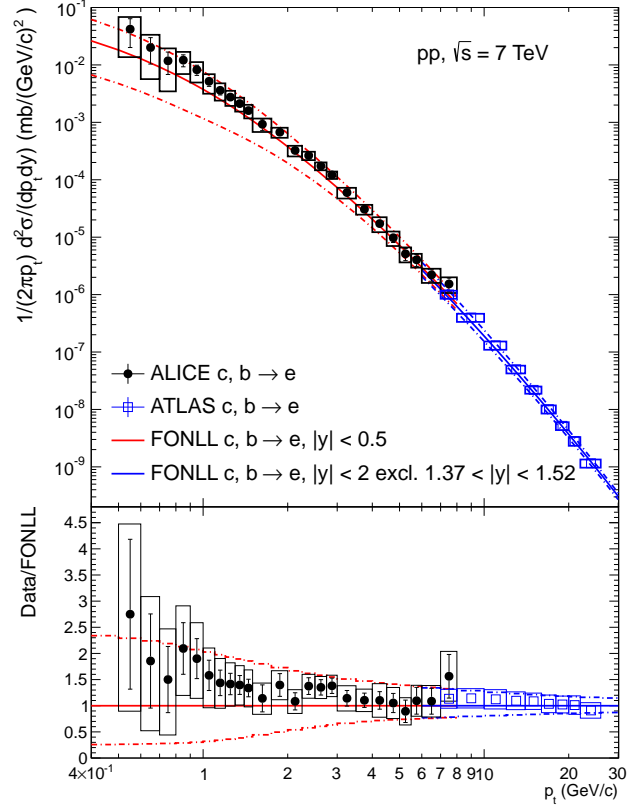


Figure 2: Invariant differential production cross sections of electrons from heavy-flavour (charm and beauty) decays measured by ALICE [3], and ATLAS [4] in pp collisions at $\sqrt{s} = 7$ TeV. The measurements are compared to a FONLL pQCD calculation.

hadron decay electron yield is determined. The result is shown in Fig. 1 (bottom). This is a first measurement of this type done in pp collisions in ALICE. The data sample, corresponding to an integrated luminosity of 14.6 nb^{-1} , was chosen because an EMCal trigger was used to select electrons above a cluster energy threshold of 3 GeV/c.

Beauty hadrons have in average a longer lifetime ($c\tau \approx 500 \mu\text{m}$) than charm hadrons and other background sources, therefore the electrons from their semi-leptonic decays have a larger impact parameter with respect to the primary interaction vertex. The silicon vertex detector of ALICE, the Inner Tracking System (ITS), provides the information on the track impact parameter with high spatial resolution, and an analysis based on the electron separation from the primary interaction is possible. This approach was used in the analysis of the pp data recorded at $\sqrt{s} = 7$ TeV, to measure the p_t -differential cross section of electrons from beauty hadron decays only. First results were presented in [9] and discussed in detail in [10].

Results from the electron analyses at mid-rapidity, at this conference, focused on measurements in pp collisions. A first look at the nuclear modification factor of electrons from heavy-flavour hadron decays was presented in [9].

3. Semi-leptonic decays of heavy-flavour hadrons at forward-rapidity

An analogous measurement of heavy-flavour hadron semi-leptonic decays can be performed at forward rapidity in ALICE, by reconstructing single muon tracks in the muon spectrometer. This consists of a passive front absorber, tracking chambers, and trigger chambers located after an iron filter, and covers the pseudorapidity range $-4 < y < -2.5$.

Muons are identified by requiring that a track reconstructed in the tracking chambers matches a corresponding track segment in the trigger chambers, to reject most of the reconstructed hadrons, stopped in the iron wall. For the candidate muons, the Distance-of-Closest-Approach (DCA) to the primary vertex is inspected, in order to remove fake tracks and tracks from beam-gas interactions. The remaining background contribution consists of muons from the decay in flight of light hadrons. In the case of proton-proton collisions, the contribution from light hadron decays can be safely estimated with Monte Carlo simulations, and it is then subtracted from the measured inclusive spectrum.

This analysis strategy was applied to reconstruct the p_t -differential production cross section of muons from heavy-flavour hadron decays in pp collisions both at $\sqrt{s} = 7$ TeV [11], and at 2.76 TeV. The latter result was newly presented at this conference and reported in detail in these proceedings [12] and in the publication [13]. The resulting cross section is compared to a FONLL prediction for the summed contribution from charm and beauty hadron decays, and is shown in Fig. 3. The theoretical prediction describes well the data.

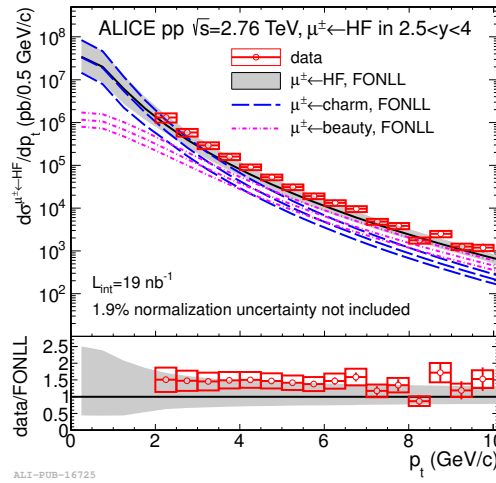


Figure 3: Production cross section of muons from heavy-flavour hadron decays measured in proton-proton collisions at $\sqrt{s} = 2.76$ TeV [12, 13]. The measurement is compared to a FONLL prediction [5, 6]. The ratio data to FONLL is shown in the lower panel.

A simple Monte Carlo approach is however not sufficient for Pb–Pb collisions, where medium effects are expected to affect the light hadron spectra. A data driven method is used, which takes pion and kaon distributions measured in the ALICE central barrel and extrapolates them to forward rapidities. A $\pm 100\%$ systematic uncertainty is assigned in this step, because of the unknown rapidity dependence of the medium effects on the light hadrons. The extrapolated spectra are then used to generate the decay muons in a full simulation of the detector setup. The systematic uncertainty on the background contribution which is subtracted allows for the application of this method for transverse momentum values above 4 GeV/c (2 GeV/c in pp collisions).

Pb–Pb collisions at $\sqrt{s_{NN}} = 2.76$ TeV recorded in Fall 2010 were analyzed and the data driven method was used to obtain a p_t spectrum of muons from heavy-flavour hadron decays for different centrality intervals of the ion-ion collisions. 16.6 million minimum bias trigger events were analyzed, for an integrated luminosity of $2.7 \mu\text{b}^{-1}$. The spectra were used to calculate the nuclear modification factor R_{AA} , defined in equation 1. The result is shown in Fig. 4, on the left for the 10% most central collisions, and on the right for the 40–80% peripheral collisions. A strong suppression (by a factor 3–4) of the muons from heavy-flavour hadron decays can be seen in the most central collisions, and is independent on the muon transverse momentum in the measured range. The suppression is much reduced in the peripheral collisions where lower energy densities are reached.

The nuclear modification factor measured in the most central collisions (Fig. 4, left) is compared to model predictions. First of all the possible effect of nuclear shadowing is estimated by using perturbative calculations by Mangano, Nason and Ridolfi [14] and the EPS09NLO [15] parameterization of the shadowing. This initial state effect reduces the parton distribution functions for partons carrying a fraction of the nucleon momentum smaller than 10^{-2} . The calculation is represented by the grey dotted-dashed curve on top, labelled NLO: the shadowing effect is small and the comparison to the data suggests the strong suppression to be dominantly a final state effect.

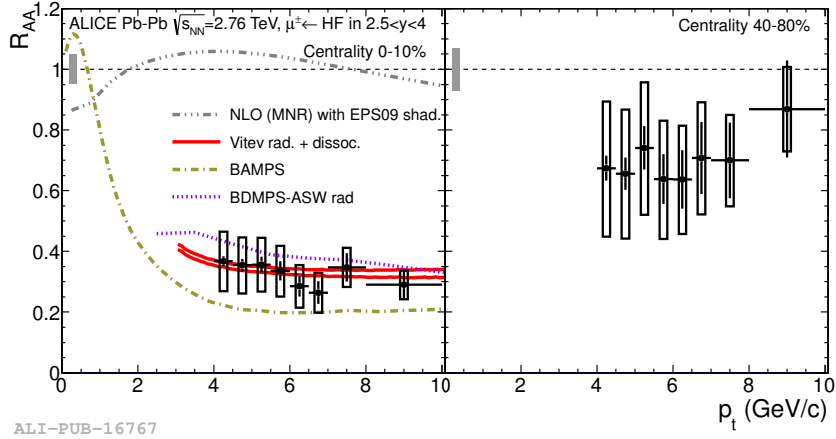


Figure 4: Nuclear modification factor as a function of the transverse momentum of the muons from heavy-flavour hadron decays, in the 0-10% most central collisions (left) and in the 40-80% peripheral collisions (right) [12, 13]. The models compared to the data are discussed in the text.

The other curves shown in the same panel represent the nuclear modification factor calculated with models which implement collisional (BAMPS) [16], radiative (BDMPS-APW) [17], and radiative with in-medium hadron formation and dissociation [18] energy loss. Good agreement is found in the two cases where radiative energy loss is included, while BAMPS underestimates the muon R_{AA} . For a more detailed description and discussion of the muon results, see [11, 12, 13].

4. Hadronic decays of charm hadrons

Hadrons containing a charm quark can be selected by fully reconstructing their decays with only hadrons in the final state. Charged tracks are reconstructed and identified at mid-rapidity in the ITS, the TPC and the TOF detectors, and combined into candidate charm particles with an invariant mass analysis. The possibility to detect charm signals via exclusive reconstruction of hadronic decay channels with very large statistics was largely improved at the LHC by the much increased heavy-flavour production cross sections compared to collisions at lower energy, and thanks to the new generation of silicon vertex detectors. ALICE is especially well equipped for these measurements because, in addition to the high resolution track and vertex reconstruction, it also profits from very good particle identification over a large momentum range. The combinatorial background rejection is largely improved by the use of the information on the particle identification. The issue is particularly important in the high multiplicity environment of central Pb–Pb collisions, where a variety of decay channels could be reconstructed by ALICE.

4.1. Charm-hadron production cross section in pp

The main decay channels studied in ALICE are: $D^0 \rightarrow K^- \pi^+$, $D^+ \rightarrow K^- \pi^+ \pi^+$, $D^{*+} \rightarrow D^0 \pi^+$. Via these decay channels, the p_t -differential production cross section for prompt charm mesons (where prompt indicates that they are produced in the primary interaction and do not come from the decay of a beauty hadron) has been measured in pp collisions at $\sqrt{s} = 7$ TeV and at 2.76 TeV, as reported in [19] and [20], respectively. As in the case of the semi-leptonic decay measurements, the resulting production cross sections are well described by pQCD predictions, both from FONLL [5, 6, 7] and from a massive variable flavor number scheme (GM-VFNS [21, 22]).

The p_t -differential production cross sections were extrapolated to the full phase space to determine the total $c\bar{c}$ production cross section at the two collision energies [20].

Other charm hadrons are investigated in pp collisions. A measurement of the D_s production cross section, in the decay channel $D_s \rightarrow K^+ K^- \pi^+$, was presented [23, 24]. A signal is observed for the Λ_c baryon in two decay channels: $p K^- \pi^+$ and $p K_s^0$.

The variety of measured charm hadrons and decay channels provide a stringent cross-check of all heavy-flavour measurements. The investigation of the Λ_c baryon is very interesting in view of future possibilities to study in heavy-ion collisions the meson to baryon ratio also in the charm sector.

4.2. Nuclear modification factor of charm hadrons

The reconstruction of the hadronic decays of charm hadrons in Pb–Pb collisions at $\sqrt{s_{NN}} = 2.76$ TeV is a challenging task, because of the high combinatorial background, due to the very high track multiplicities. Figure 5 shows the invariant mass distributions for the decay $D^0 \rightarrow K^- \pi^+$ in three different p_t bins.

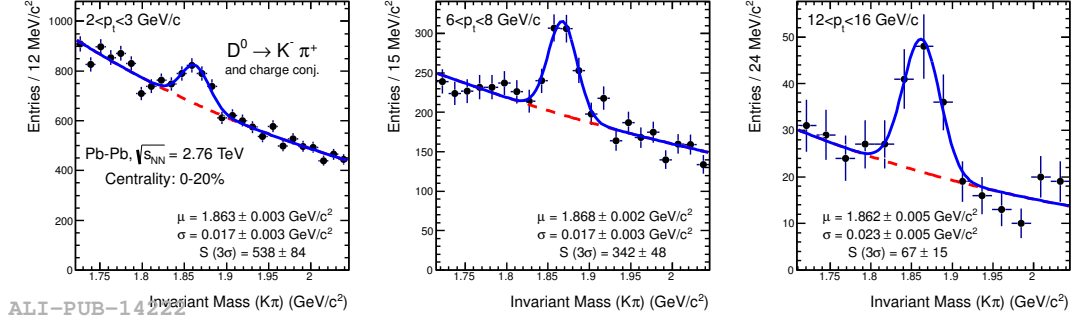


Figure 5: Invariant mass distributions for D^0 candidates in three p_t intervals for the 0–20% most central Pb–Pb collisions [25].

Also in Pb–Pb collisions the three main D meson decay channels discussed in 4.1 are reconstructed, and differential p_t spectra are measured over the range $2 < p_t < 16$ GeV/c. Results from the 2010 sample of Pb–Pb minimum bias events, for an integrated luminosity of about $2.1 \mu\text{b}^{-1}$, are presented. Prompt D meson yields are obtained by subtracting the contribution of D mesons from B decays. This is evaluated using the FONLL estimate of the beauty production cross section, and the $B \rightarrow D$ decay kinematics. The contribution is then renormalized by the average nuclear overlap function in each centrality interval, and the nuclear modification factor of the D mesons from B decays, assuming it equal to that of prompt D mesons. All details of the analysis in Pb–Pb can be found in [25].

The prompt D^0 , D^+ , and D^{*+} p_t -differential yields in the 0–20% and 40–80% centrality classes are then used to compute the nuclear modification factor, shown in Fig. 6 as a function of the D meson transverse momentum.

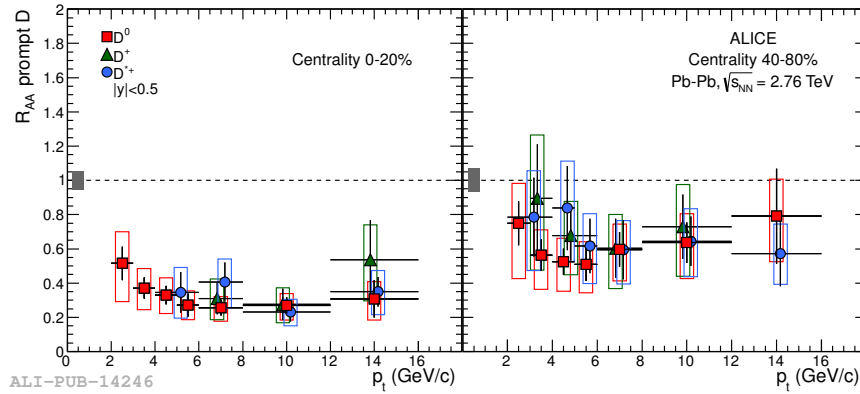


Figure 6: Nuclear modification factor for prompt D^0 , D^+ , and D^{*+} as a function of the meson transverse momentum, in the 0–20% (left) and 40–80% (right) centrality intervals [25].

The results from the three D mesons are compatible, and show a suppression by a factor of 3–4 in the most central events, with no significant dependence on the transverse momentum above 5 GeV/c. The suppression factor increases going from more peripheral to more central collisions.

The averaged D meson R_{AA} is compared with a calculation including the effects of nuclear shadowing, based on perturbative calculations by Mangano, Nason and Ridolfi [14] and the EPS09NLO [15] parameterization, similarly to the muon case discussed in the previous section. The comparison is shown in Fig. 7 (left): above 6 GeV/c, the shadowing-induced effect on R_{AA} is small and cannot explain the measurement. This suggests once again that the strong suppression of heavy flavours observed in data is a final state effect.

The parton energy loss in the medium is described by a number of different models, which calculate the charm nuclear modification factor. Some of the predictions are shown in Fig. 7 (right). As commented in the muon case, models including radiative components of the energy loss describe reasonably well the measured suppression.

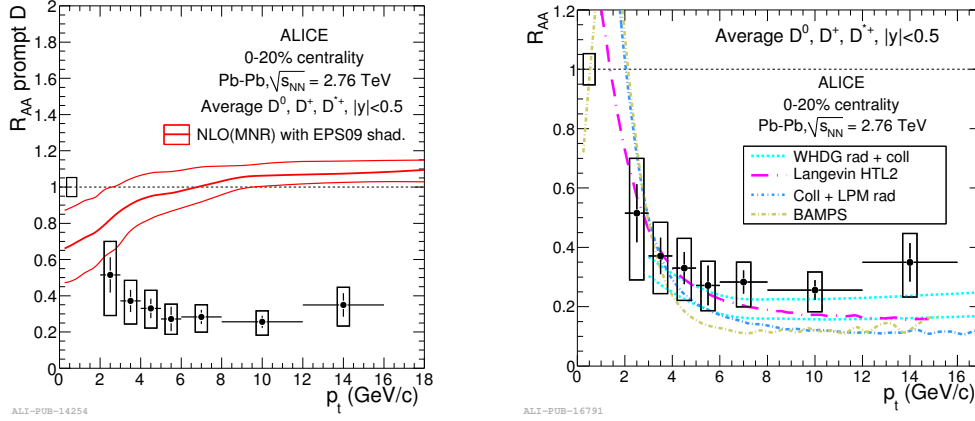


Figure 7: The average D meson R_{AA} is compared with a calculation of nuclear shadowing (left) [25] and various parton energy loss models: WHDG rad + coll [26], Langevin HTL2 [27], Coll + LPM rad [28, 29], and BAMPS [16].

4.3. Elliptic flow of D mesons

In addition to the parton energy loss in the QGP, another very important question about heavy quarks concerns their degree of thermalization inside the medium and the participation to its collective motion. A study of the azimuthal anisotropy of the prompt D meson production brings information, at low transverse momentum, on the charm thermalization and, at high momentum, on the path-length dependence of the parton energy loss. The dominant component of the anisotropic distribution is called elliptic flow and is commonly quantified by the second coefficient, v_2 , of a Fourier decomposition of the azimuthal distribution of observed particles relative to the event-plane angle. The flow measurement was made possible by the larger statistics recorded in the 2011 Pb–Pb data taking period. A centrality trigger enhanced the statistics in the 30–50% centrality interval to almost 10^7 events.

The event plane is determined from the distribution of charged tracks in the TPC. The elliptic flow of D^0 mesons was calculated by comparing the signal found in two complementary angular regions of the transversal plane, one called “in plane”, the other “out of plane”. The invariant mass analysis provides the number of signal candidates found in the two regions (N_{IN} , N_{OUT}) and the elliptic flow can be obtained as: $v_2 = \frac{\pi}{4} \frac{N_{IN} - N_{OUT}}{N_{IN} + N_{OUT}} \frac{1}{r}$, where r is the event plane resolution. Details of this analysis are discussed in [30].

The resulting v_2 of D^0 mesons as a function of the transverse momentum is shown in Fig. 8 (left). A non-zero elliptic flow (with a 3σ significance) is found in the range $2 < p_t < 6$ GeV/c. The result is of the same magnitude of the v_2 of charged tracks measured in ALICE, within the large uncertainties. The D^0 result is confirmed by a similar measurement with the D^+ in the same centrality bin, and by different methods to compute v_2 . The figure on the right side shows a comparison of the measured elliptic flow with predictions by the same models already used in Fig. 7 in comparison to the D meson R_{AA} . With the availability of the many results on nuclear modification factors and elliptic flow of heavy flavours, it is now very important that theoretical models provide a simultaneous and coherent description of the transport and energy loss of the heavy quarks in the medium.

5. Summary

After the first two years of data taking with proton-proton and Pb–Pb collisions at the LHC, at the highest ever reached energies, ALICE has presented a very rich collection of physics results on the production of heavy quarks in hadronic collisions, and their modification in the presence of the strongly-interacting, deconfined medium produced in heavy-ion collisions. Production cross sections measured in pp both for charm and for beauty are very well described

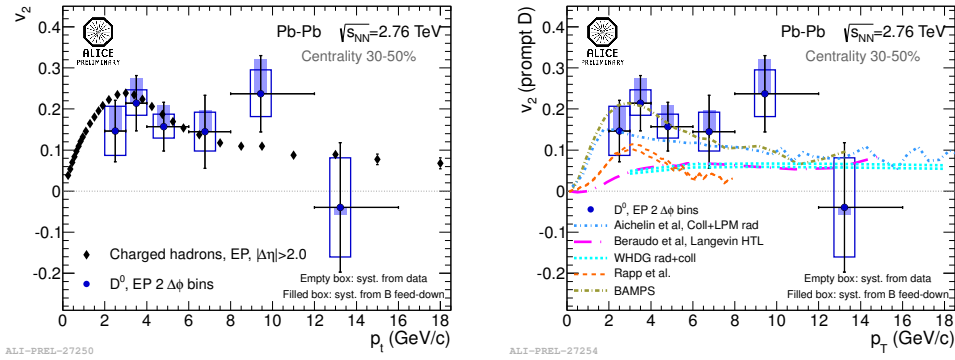


Figure 8: (Left) D^0 elliptic flow measured in the 30-50% centrality class [30], compared to the elliptic flow of charged particles measured in ALICE [31]. (Right) Comparison to the same models for which a description of the D meson R_{AA} was given in Fig. 7.

by pQCD predictions, and provide the reference for measurements in Pb–Pb. In the most central heavy-ion collisions, a strong suppression by a factor 3–4 is measured for heavy-quark hadrons, in the intermediate p_t region. The suppression exhibits a clear centrality dependence and no strong p_t dependence in the range $5 < p_t < 15$ GeV/c. A non-zero elliptic flow of D mesons is measured at low transverse momentum, in semi-central collisions. One of the main goals for the near future is to extend the p_t range of the measurements, both to higher momenta, and to very low p_t where very interesting physics is to be understood. At low momentum, in fact, the heavy-flavour production cross section is largest and, in heavy-ion collisions, the quenched heavy-flavour hadrons have to accumulate. Furthermore, it will soon be possible to isolate and investigate the beauty component also in Pb–Pb collisions.

References

- [1] M. L. Miller, K. Reygers, S. J. Sanders, and P. Steinberg. *Ann.Rev.Nucl.Part.Sci.*, 57:205–243, 2007.
- [2] K. Aamodt et al. *JINST*, 3:S08002, 2008.
- [3] B. Abelev et al. arXiv:1205.5423 [hep-ex].
- [4] G. Aad et al. *Phys. Lett.*, B707:438–458, 2012.
- [5] M. Cacciari, M. Greco, and P. Nason. *JHEP*, 9805:007, 1998.
- [6] M. Cacciari, S. Frixione, and P. Nason. *JHEP*, 0103:006, 2001.
- [7] M. Cacciari et al. arXiv:1205.6344 [hep-ph].
- [8] B. Biritz. *Nucl.Phys.*, A830:849C–852C, 2009.
- [9] S. Masciocchi for the ALICE Coll. *J.Phys.*, G38:124069, 2011.
- [10] M. Kwon for the ALICE Coll. These proceedings. arXiv:1208.5411 [nucl-ex].
- [11] B. Abelev et al. *Phys.Lett.*, B708:265–275, 2012.
- [12] D. Stocco for the ALICE Coll. These proceedings. arXiv:1208.6171 [nucl-ex].
- [13] B. Abelev et al. arXiv:1205.6443 [nucl-ex].
- [14] M. L. Mangano, P. Nason, and G. Ridolfi. *Nucl.Phys.*, B405:507–535, 1993.
- [15] K.J. Eskola, H. Paukkunen, and C.A. Salgado. *JHEP*, 0904:065, 2009.
- [16] J. Uphoff, O. Fochler, Z. Xu, and C. Greiner. These proceedings. arXiv:1205.4945 [nucl-ex].
- [17] N. Armesto, A. Dainese, C. A. Salgado, and U. A. Wiedemann. *Phys.Rev.*, D71:054027, 2005.
- [18] R. Sharma, I. Vitev, and B. Zhang. *Phys.Rev.*, C80:054902, 2009.
- [19] B. Abelev et al. *JHEP*, 1201:128, 2012.
- [20] B. Abelev et al. *JHEP*, 1207:191, 2012.
- [21] B.A. Kniehl, G. Kramer, I. Schienbein, and H. Spiesberger. *AIP Conf.Proc.*, 792:867–870, 2005.
- [22] B.A. Kniehl, G. Kramer, I. Schienbein, and H. Spiesberger. *Eur.Phys.J.*, C41:199–212, 2005.
- [23] C. Geuna for the ALICE Coll. These proceedings. arXiv:1209.0382 [hep-ex].
- [24] B. Abelev et al. arXiv:1208.1948 [hep-ex].
- [25] B. Abelev et al. arXiv:1203.2160 [hep-ex].
- [26] W.A. Horowitz and M. Gyulassy. *J.Phys.*, G38:124114, 2011.
- [27] W.M. Alberico, A. Beraudo, A. De Pace, A. Molinari, M. Monteno, et al. *Eur.Phys.J.*, C71:1666, 2011.
- [28] P.B. Gossiaux, R. Bierkant, and J. Aichelin. *Phys.Rev.*, C79:044906, 2009.
- [29] P.B. Gossiaux, J. Aichelin, T. Gousset, and V. Guio. *J.Phys.*, G37:094019, 2010.
- [30] G. Ortona for the ALICE Coll. These proceedings. arXiv:1207.7239 [hep-ex].
- [31] K. Aamodt et al. *Phys.Rev.Lett.*, 105:252302, 2010.